Published in final edited form as:
Cancer Epidemiol Biomarkers Prev. 2008 November ; 17(11): 3090–3097. doi: 10.1158/1055-9965.EPI-08-0170.

An Automated Approach for Estimation of Breast Density

John J. Heine[1], **Michael J. Carston**[2], **Christopher G. Scott**[2], **Kathleen R. Brandt**[2], **Fang-Fang Wu**[2], **V. Shane Pankratz**[2], **Thomas A. Sellers**[1], and **Celine M. Vachon**[2]
[1]H. Lee Moffitt Cancer Center and Research Institute, Tampa, Florida

[2]Mayo Clinic College of Medicine, Rochester, Minnesota

Abstract

Breast density is a strong risk factor for breast cancer; however, no standard assessment method exists. An automated breast density method (ABDM) was modified and compared with a semi-automated user-assisted display method (CM) and the Breast Imaging Reporting and Data System (BI-RADS) four-category tissue composition measure for their ability to predict future breast cancer risk. The three estimation methods were evaluated in a matched breast cancer case (n=372) control (n=713) study at the Mayo Clinic using digitized film mammograms. Mammograms from the craniocaudal (CC) view of the noncancerous breast were acquired on average seven years before diagnosis. Two controls with no prior history of breast cancer from the screening practice were matched to each case on age, number of prior screening mammograms, final screening exam date, menopausal status at this date, interval between earliest and latest available mammograms, and residence. Both Pearson linear correlation (R) and Spearman rank correlation (r) coefficients were used for comparing the three methods where appropriate. Conditional logistic regression was used to estimate the risk of breast cancer (odds ratios [ORs] and 95% confidence intervals [CIs]) associated with the quartiles of percent density (ABDM, CM) or BI-RADS category. The area under the receiver operator characteristic curve (AUC) was estimated and used to compare the discriminatory capabilities of each approach. The continuous measures ABDM and CM were highly correlated with each other (R=0.70) but less with BI-RADS (r=0.49 for ABDM and r=0.57 for CM). Risk estimates associated with the lowest to highest quartiles of ABDM were greater in magnitude (ORs: 1.0[ref], 2.3, 3.0, 5.2, p-trend<0.001) than the corresponding quartiles for CM (ORs: 1.0[ref], 1.7, 2.1 and 3.8; p-trend<0.001) and BI-RADS (ORs: 1.0[ref], 1.6, 1.5, 2.6; p-trend<0.001) methods. However, all methods similarly discriminated between case and control status: AUCs were 0.64, 0.63 and 0.61 for ABDM, CM and BI-RADS, respectively. The ABDM is a viable option for quantitatively assessing breast density from digitized film mammograms.

Keywords

Automated density; breast density; methodology

Introduction

Breast density is a significant breast cancer risk factor (1). Various methods have been investigated for measuring breast density, but to date, no accepted measurement standards exist (2). The Cumulus user-assisted method (CM) based on soft-copy display intensity thresholding

Requests for reprints: Celine M. Vachon, Mayo Clinic College of Medicine, Charlton 6-239, 200 First St. SW, Rochester, MN 55905. Phone: 507-284-9977; Fax: 507-266-2478. E-mail: E-mail: vachon.celine@mayo.edu.

Disclosure of Potential Conflicts of Interest
No potential conflicts of interest were disclosed.

(3–5) is considered the *de facto standard*. It and other similar techniques (6) generate quantitative measures that have shown, with repeatability, to correlate with breast cancer risk (1). However, subjective estimates including the American College of Radiology (ACR) Breast Imaging Reporting and Data System (BI-RADS) four-category tissue composition description and subjective classifications of breast density have also demonstrated consistent associations with breast cancer risk (1). Current density estimation methods show strong associations with risk (1), but they remain time intensive, require operator training (7), and may not be comparable across studies. Thus, *an automated* quantitative metric for assessing breast density is needed that does not require operator interaction. We use the term "automated" to describe the method of breast density estimation without regard to the digitization or image formation process. This includes the "automated" labeling of pixel(s) within a given image and the method used for summarizing the labeled pixels to provide a density estimate.

Current computer based methods for density estimation can be loosely categorized into two groups: 1) those that compensate for acquisition influences resulting from the inter-patient variation in the X-ray exposure, target-filter combination, compression height and X-ray generation voltage (8–13), and 2) those that operate on the image data without considering the acquisition influences (3–6,14). The acquisition compensation techniques are under various stages of development and testing for both film (8,10,13) and full-field digital mammography (FFDM) applications (9,11,12). Whether considering the acquisition or not, film based approaches require a digitizing step before their application in contrast in those techniques intended for FFDM applications. Few acquisition based approaches have been replicated or validated using breast cancer as an endpoint. A recent study comparing the SMF (Standard Mammogram Format) volumetric method to CM for its ability to discriminate cancer status found CM to be more strongly associated with risk (15). Other non-acquisition-based approaches that rely on some form of quantitative summary feature (i.e. skewness, kurtosis, etc.) derived from the digitized film data resulted in weaker risk associations than the CM measure (14,16).

Because breast density is an important risk factor whose magnitude of association is stronger than the majority of established breast cancer risk factors (17), it may improve risk prediction models for breast cancer (18–20). However, breast density has not been routinely incorporated into clinical risk prediction, perhaps due to lack of standardized estimates and the technical expertise required to generate such estimates in the clinical setting. An estimate of density that could be automatically applied to digitized film and digital data from FFDM would help alleviate these barriers.

Although the majority of mammography clinics in the US continue to use film mammography, FFDM is increasing as the screening standard (21) due to its superior sensitivity in dense breasts (22). In the interim, while both FFDM and film coexist, assessing breast density from digitized film will continue to be relevant due to the large film archives with serial data and well-annotated clinical outcomes and the ability to translate clinically relevant findings identified from film to digital mammography.

In this work, a previously described automated breast density method (ABDM) developed for digitized film applications (23) was modified and compared with the continuous CM measure and the radiologists' classifiction of BI-RADS tissue composition. The correlation of the three estimates and their ability to discriminate breast cancer was evaluated on digitized films within a breast cancer case-control study.

Materials and Methods

Study Population and Image Data

The case-control study used for this work was described in detail previously (24). Eligible participants provided research authorization for medical record studies at the Mayo Clinic. Informed consent for this case-control study was waived. All patient data was retrospectively obtained through medical records, clinical databases or mammogram films; no patients were contacted for this study. The Mayo Clinic Institutional Review Board approved the study protocol.

Breast cancer cases (n=372) diagnosed from 1997–2001 were ascertained from the Mayo Clinic mammography screening practice in Rochester, Minnesota. Eligible cases were at least 50 years old at diagnosis, had at least two prior screening mammograms performed at the Mayo Clinic two years prior to diagnosis (or corresponding exam date), and lived within a 120-mile radius. Both invasive (n=300) and in situ (n=72) breast cancers were included. Multiple mammograms prior to diagnosis were retrospectively collected to investigate changes over time in mammographic density and breast cancer risk (for another study) as well as to establish a population of women having routine mammograms. Two controls from the screening practice with no prior history of breast cancer were matched to each case on age, final screening exam date, menopausal status at final exam date, time between earliest and latest mammograms, number of prior screening mammograms, and residence. Since mammograms are only retained for ten years at the Mayo Clinic, the earliest mammogram available during this period was defined as the baseline image. The baseline mammogram available for both cases and controls was used for the analyses. Medical records provided weight, height, and postmenopausal hormone therapy use for all serial mammogram dates; the measures closest to the earliest mammogram dates were used (24). Weight and height were available within 1 week of the baseline mammogram for 85% and 68% of participants, respectively. Postmenopausal hormone therapy information (ever/never use) was available for 84% of participants. A mammography database, which is based on self-reported information gathered at each mammogram (including menopause status, family history in first-degree relatives, age at first birth, number of births, prior biopsies and prior breast cancer), provided all remaining patient information.

Mammograms were digitized with a Kodak Lumiscan 75 scanner (LS-75) with 12-bit grayscale pixel depth. The pixel size was 0.130×0.130 mm^2 for both the 18×24 cm^2 and 24×30 cm^2 films. All four views — left and right mediolateral oblique (MLO) view and left and right craniocaudal (CC) view — were digitized for each woman. The film background in each image was manually blacked out to protect patient privacy and increase data compression rates when archiving the data. For both the MLO and CC views, an edge detection program automatically segmented the breast tissue from the background image and the delineation was manually checked by the reader for accuracy. The MLO view additionally required the manual removal of the pectoral muscle. This process was the same for the estimation of percent density by the CM and ABDM measures. In practice, the CC views are preferable for automated processing since they do not require removal of the pectoral muscle (25). However we included the modified MLO views as another assessment of the ABDM statistical decision process.

The three measures for estimation of breast density are described below.

User-Assisted Thresholding Measure—The semi-automated user-assisted display method (CM) is a user-guided process that requires manual segmentation and intensity thresholding to estimate percent mammographic density (3–5), referred to as PD in this report. The operator set two thresholds: one delineated the breast from the background (done automatically as defined above) and the other set the threshold between dense and non-dense

pixels (3). The application computed the total area and dense area and then calculated PD by dividing the dense area by total area, which was a unit-less ratio or proportion. Batch files were created for both cases and controls with randomly assigned views and sides within person (26). A single technician analyzed all images for consistency. This technician repeatedly demonstrated high reliability (R>0.90) while reading over 500 duplicate images across varying time frames.

The Automated (ABDM) Approach—The ABDM (23) is an extension of earlier work that analyzed digitized mammograms after applying digital filtering (27). This work showed a strong correspondence between areas of increased breast density in the raw image (bright image areas) and areas of increased pixel variance within a special type of high-pass filtered representation (23) of the raw image. In the original developmental work (23,27), a deconvolution operation defined the special high pass filter application, which is a pre-whitening (PW) filter. A PW operation *removed* the Fourier spectral form of the raw image leaving a zero mean noise field with little spatial correlation. The PW operation was applied by first estimating the Fourier spectral form for a given raw image and then constructing a filter to remove the form. In the work presented here, a wavelet high pass filter was used in place of the deconvolution operation because it was faster, did not require estimating the raw image spectral form, and produced similar breast density results in the preliminary (training) analysis. The wavelet filter methods used here were discussed in detail previously (28,29). The ABDM operated by applying a statistical test within the filtered image by scanning a small search window (defined below) across the image. Within each window positioned at a given location, a statistical test based on the filtered image variance, was applied to detect regions corresponding to brighter regions in the raw image. The statistical test was based on chi-square analysis, which followed from the spatial statistical qualities of the filtered image representation. The ABDM produced a similar area-based measure (a ratio) as the PD, which was summarized and normalized in the same way once a given image was binary labeled by the outcomes of the statistical tests. The ABDM measure will be referred to as PD_A in this report.

Briefly, we first converted the image data from the LS-75 digitizer to the digital representation from the DBA digitizer (DBA Systems, Melbourne FL) used in the earlier work (23,27,28). Both systems used digitized film data, but the LS-75 is linear in its optical density pixel value relation while the DBA is exponential. This involved linearly transforming the LS-75 data to optical density (OD) units and then converting to the older representation using the relation: *original representation* = 29891exp (−2.36OD). Next, the breast region field of view was automatically located relative to the off-breast background. This was done by taking all pixels with *pixel values* >0, since the off-breast background had already been blacked out as described above. Finally, the ABDM was applied to the breast field of view of the filtered image. This involved automatically dividing the filtered image into a grid of 4 × 4 pixel boxes (the box is the search window) and then applying an automated statistical decision to each grid location so that all pixels within a given grid were either labeled as fatty tissue or dense tissue (in the first stage). A second iteration was performed to refine the labeling of fat and dense tissue, resulting in the density labeled ABDM output image and overall proportion of density (in the second stage). The two-stage detection scheme was discussed in considerable detail in the original report (23).

To establish parameters for the ABDM algorithm, a set of mammogram images on healthy women (training data) was obtained from a similar Caucasian population. The ABDM has two adjustable detection parameters corresponding to each detection stage. These values were estimated via correlation analysis with the CM for the images in the training set. The parameters were fixed when a maximum correlation was achieved.

BI-RADS Tissue Composition Descriptions—The BI-RADS four-category tissue composition assessment has been part of standard clinical practice at the Mayo Clinic since 1992. Mayo Clinic attending radiologists classified BI-RADS tissue composition into one of four categories as defined in the BI-RADS lexicon (ACR-third edition): 1) the breast is almost entirely fat; 2) there are scattered fibroglandular densities; 3) the breast tissue is heterogeneously dense, which may lower the sensitivity of mammography; and 4) the breast is extremely dense, which could obscure a lesion on mammography. These ratings convey the relative possibility that a lesion may be obscured in mammography. All four mammogram views (CC and MLO for ipsilateral and contralateral sides) contribute to the assessment of BI-RADS breast composition. In our study, we used the BI-RADS estimates that experienced radiologists assessed in the clinical setting. These radiologists did not systematically assess BI-RADS composition for this study, but the BI-RADS rating has shown adequate inter-observer validity (30). The BI-RADS estimate used in current clinical practice includes quantifying the percentage of breast density into four categories in conjunction with the above descriptors. However, due to the retrospective data collection, the BI-RADS used in our analyses followed the older convention that did not include breast density percentages.

Statistical Analysis

Prior results from this case-control study illustrated the association of PD (CM) with breast cancer was invariant to the mammogram view or (for the cases) whether the view was based on the cancerous or non-cancerous breast (24). Thus, we restricted our evaluation of the methods for percent density estimation in this report to the non-cancerous breast and present results for both the CC and MLO views.

Summaries of the distribution of matching variables were presented as means and standard deviations or counts and percentages. The distributions of both PD and PD_A were approximately normally distributed in this population. The correlation of PD_A with PD was estimated using the Pearson correlation coefficient (R) for the entire range of breast density values. The correlations between MLO and CC view for both PD and PD_A were also calculated using this method. Correlation of PD and PD_A with the BI-RADS classification were estimated using the Spearman correlation coefficient (r) due to the discrete nature of the BI-RADS measure. Linear regression methods and corresponding R-square values (R^2) evaluated the apparent curvilinear relationship between PD and PD_A. Conditional logistic regression examined the associations of the three methods of mammographic density estimation with breast cancer. PD and PD_A were examined as a categorical measure based on quartiles of their distributions among controls and a continuous measure reflecting an increase of one standard deviation. For BI-RADS, the four-category classification was used. Odds ratios and 95% CIs were estimated for these measures of mammographic density. All models were adjusted for age and body mass index (BMI), which was calculated as weight (kg)/height (m^2).

The strength of association for the three methods with breast cancer was summarized with a modified c-statistic, also known as area under the receiver operator characteristic curve (AUC). C-statistics reflect how often a model correctly identifies the case in a random case control pair and range from 0.5 (random chance) to 1.0 (perfect prediction). To take advantage of the case-control matching, only pairs occurring within matched sets of cases and controls were used in the calculation of the c-statistic (31).

Results

The average time interval between the earliest mammogram and the diagnosis of cancer (or corresponding exam date) was 7.1 + 1.5 years for cases and 7.0 ± 1.5 years for controls; these intervals were greater than 5 years for over 90% of the participants (Table 1). As described previously, the cases and controls were closely matched as shown by the similarities of age,

number of screening mammograms, interval between mammograms, menopausal status and residence (Table 1) (24). Figure 1 illustrates CC mammograms from three women in the LS-75 representation used for PD (Fig. 1a) compared with the converted digital DBA representation used for PD_A (Fig. 1b). The corresponding PD (Fig. 1a) and PD_A (Fig. 1b) values are provided in the figure legends. The converted images appear to have more contrast than the LS-75 representation. The distinct difference between the representations is exemplified by the degree of bright tissue near the breast-background border region in the LS-75 representation.

For the CC views, the correlation of PD-PD_A was R = 0.70 (Fig 2), for PD_A-BI-RADS, r = 0.49 (Table 2), and PD-BI-RADS, r = 0.57 (Table 2). Figure 2 illustrates a slight curvilinear association between the PD_A and PD. Inclusion of a quadratic term entered in the linear regression model improved the model fit, increasing R^2 from 0.45 to 0.53 for the CC view (MLO view R^2: 0.42 to 0.50). The range of density was substantially reduced for the ABDM (6%–32%) compared with the CM (0%–80%). Consequently, the variance of the ABDM is reduced as well (Table 3). The correlation of PD between the CC and MLO views was higher (R=0.90) than the between-view correlation for PD_A (R=0.78).

All three measures showed expected associations with established breast cancer risk factors, including inverse associations with age, BMI, parity, postmenopausal status and never postmenopausal hormone therapy use, although the parity associations were more pronounced for PD compared to PD_A or BI-RADS (Table 3). Table 4 shows associations between these measures with breast cancer. Positive associations between percent density and breast cancer were found with all measures and both views. The risk associations for all three density estimates were comparable. PD_A had higher odds ratios (OR) and wider confidence intervals than the PD and BI-RADS classification; however, the AUCs for all methods were virtually identical (Table 4). In addition, the AUCs for the continuous PD and PD_A measures (per one standard deviation (SD)) were similar to those from the models that evaluated quartiles of PD and PD_A (Table 4). There was no evidence of a quadratic association for either the continuous PD or PD_A (data not shown).

Discussion

The results of the current study demonstrate that ABDM is a viable option for estimating breast density. PD_A is correlated with the PD and BI-RADS estimates, and the risk estimates for quartiles of PD_A are comparable to reported estimates from a variety of studies (1). Also, PD_A discriminates between case-control status as well as PD or BI-RADS.

Incorporation of breast density into risk assessment models could provide a woman with an improved estimate of her absolute breast cancer risk. Accurate knowledge of individual risk results in more informed clinical decisions regarding interventions and screening frequency and can provide a reference of where a woman lies with respect to average risk (32). Data shows that clinical radiologists' BI-RADS categorization, together with age and ethnicity, provides as much information as the existing Gail model for breast cancer risk prediction (18), underscoring its relative importance as a marker of risk. Two recent studies evaluated the addition of breast density to risk prediction models and found some improvement of fit (19, 20). To facilitate the incorporation of breast density into clinical practice and decision making, the ABDM could be added to existing computer-assisted diagnostic systems (CAD) (33) currently used in clinical practice to detect suspicious areas on mammograms. This would allow for a quantitative breast density measure that is automatically and objectively generated, guaranteeing reproducible and comparable measurements across sites. Also, the ABDM would result in greater time and cost savings in comparison with user assisted or experienced observer interpretation methods.

In addition to improving absolute risk prediction, the ABDM may also be the most appropriate measure for assessing change in breast density. Change in breast density has been used as an intermediate biomarker for efficacy of interventions, such as tamoxifen or gonadotropin-releasing hormone agonist (34,35). When assessing the amount of change in density, a quantitative measure is preferable because the degree of change is limited to the resolution of the measure. We (36) and others (35,37,38) have shown that PD changes that occur in postmenopausal women are small in magnitude and could be missed if assessed solely by the BI-RADS categorical measure. Thus, for assessment of serial breast density changes especially in postmenopausal women, a quantitative estimate, such as the ABDM or CM, is preferred. Furthermore, the ABDM may be preferable for comparability of breast density change across studies and institutions since the ABDM is independent of operator while the CM requires user-defined thresholds subject to inter-reader variation.

The ABDM is currently an experimental software/approach that requires further this study, including both the training data used for initialization of the ABDM parameters and the case-control study data, were collected by one center and digitized with a single digitizer (LS-75). The ABDM requires modification to accept image data acquired from various mammogram detectors (digitized film or FFDM digital acquisition). Preliminary work (39) shows that when applying the ABDM to FFDM data, the density estimate correlates with a calibrated FFDM breast density measure (9) when applied to the same dataset. Thus, it is possible that the ABDM can be applied to FFDM data to discriminate case and control status.

While the ABDM and CM measures are correlated, the range of density was substantially narrower for the ABDM (6%–32%) when compared with the CM (0%–80%). This difference in scale is partly due to the different data representations of the LS-75 and the DBA digitizer outputs. The LS-75 raw image pixel range is compressed relative to the DBA representation. This difference, together with the way that the parameters of the ABDM - PD_A were selected to maximize its linear correlation with CM - PD, results in different scales for the two breast density quantitative estimates. However, these scale differences do not represent a serious obstacle because of the near linear relation. It would be relatively easy to either expand one scale or compress the other to obtain breast density scores that are similarly scaled. We have retained the simple estimates from each to make comparisons between the two scales similar to the way the Celsius and Fahrenheit temperature scales are compared.

On the other hand, there is little evidence indicating that either the PD or PD_A scales or the corresponding breast density representations are optimal or preferable. For example, both representations follow from binary labeling. This form of labeling implies a pixel labeled as 100% dense breast tissue within the central uniformly compressed region of the breast carries as much weight as a pixel labeled similarly in the region near the breast-background border that is not of uniform thickness. As another example, the implications in the extreme case where a breast is labeled near 100% PD would imply that the breast volume is comprised of 100% dense breast tissue, which is unlikely.

The ABDM requires a consistent method for segmenting the breast tissue from the digital image. The work presented here represents an ideal application since each image background was set to zero prior to ABDM, which made segmentation of the breast tissue trivial. This does not represent a hindrance to its application on other datasets since many fully automated routines also segment the breast tissue from the background (40–42).

The generalizability of ABDM is currently limited to film mammography, which comprises approximately 85% of mammography units in the United States (21). Developing methods for film-analysis may be questioned in light of the emerging FFDM technology, which may provide many benefits due to its digital form (43). However, film mammograms are still the

mainstream for screening, and the associated data archives that span several years are capable of supporting clinical studies. This is not generally the case for FFDM data. On the other hand, FFDM data may lend itself to acquisition standardization (or calibration) more easily than film, but the techniques for this purpose are currently works in progress (9,11,12) that warrant validation in terms of their short-term and long-term ability to produce a measure that correlates with risk. Various manufactures of FFDM systems have both raw (inverted data scales) and display data representations. Some FFDM systems allow easy access to the raw data, whereas other systems do not. Likewise, some centers discard the raw data due to storage limitations, which limits the analyses that can be performed on the FFDM images. At this time, both forms of mammography (film and the various FFDM systems) exist simultaneously, and both can assist in improving risk estimations.

Acknowledgments

We acknowledge the women within our mammography practice that provided research authorization for medical record studies.

Grant support: Department of Defense (DAMD 17-00-1-0331), National Cancer Institute (R01 CA97396 and P50 CA116201)

References

1. McCormack VA, dos Santos Silva I. Breast density and parenchymal patterns as markers of breast cancer risk: a meta-analysis. Cancer Epidemiol Biomarkers Prev 2006;15:1159–1169. [PubMed: 16775176]
2. Couzin J. Breast cancer. Dissecting a hidden breast cancer risk. Science 2005;309:1664–1666. [PubMed: 16150987]
3. Byng JW, Boyd NF, Fishell E, Jong RA, Yaffe MJ. The quantitative analysis of mammographic densities. Phys Med Biol 1994;39:1629–1638. [PubMed: 15551535]
4. Byng JW, Yaffe MJ, Jong RA, et al. Analysis of mammographic density and breast cancer risk from digitized mammograms. Radiographics 1998;18:1587–1598. [PubMed: 9821201]
5. Boyd NF, Byng JW, Jong RA, et al. Quantitative classification of mammographic densities and breast cancer risk: results from the Canadian National Breast Screening Study. J Natl Cancer Inst 1995;87:670–675. [PubMed: 7752271]
6. Ursin G, Ma H, Wu AH, et al. Mammographic density and breast cancer in three ethnic groups. Cancer Epidemiol Biomarkers Prev 2003;12:332–338. [PubMed: 12692108]
7. Prevrhal S, Shepherd JA, Smith-Bindman R, Cummings SR, Kerlikowske K. Accuracy of mammographic breast density analysis: results of formal operator training. Cancer Epidemiol Biomarkers Prev 2002;11:1389–1393. [PubMed: 12433716]
8. Highnam, R.; Brady, M. Mammographic Image Analysis. Boston, MA: Kluwer Academic Publishers; 1999.
9. Kaufhold J, Thomas JA, Eberhard JW, Galbo CE, Trotter DE. A calibration approach to glandular tissue composition estimation in digital mammography. Med Phys 2002;29:1867–1880. [PubMed: 12201434]
10. Pawluczyk O, Augustine BJ, Yaffe MJ, et al. A volumetric method for estimation of breast density on digitized screen-film mammograms. Med Phys 2003;30:352–364. [PubMed: 12674236]
11. Heine JJ, Behera M. Effective x-ray attenuation measurements with full field digital mammography. Med Phys 2006;33:4350–4366. [PubMed: 17153414]
12. Heine JJ, Thomas JA. Effective x-ray attenuation coefficient measurements from two full field digital mammography systems for data calibration applications. Biomed Eng Online 2008;7:13. [PubMed: 18373863]
13. Shepherd JA, Herve L, Landau J, Fan B, Kerlikowske K, Cummings SR. Novel use of single X-ray absorptiometry for measuring breast density. Technol Cancer Res Treat 2005;4:173–182. [PubMed: 15773786]

14. Torres-Mejia G, De Stavola B, Allen DS, et al. Mammographic features and subsequent risk of breast cancer: a comparison of qualitative and quantitative evaluations in the Guernsey prospective studies. Cancer Epidemiol Biomarkers Prev 2005;14:1052–1059. [PubMed: 15894652]
15. Ding J, Warren R, Warsi I, et al. Evaluating the effectiveness of using standard mammogram form to predict breast cancer risk: case-control study. Cancer Epidemiol Biomarkers Prev 2008;17:1074–1081. [PubMed: 18483328]
16. Byng JW, Yaffe MJ, Lockwood GA, Little LE, Tritchler DL, Boyd NF. Automated analysis of mammographic densities and breast carcinoma risk. Cancer 1997;80:66–74. [PubMed: 9210710]
17. Boyd NF, Lockwood GA, Byng JW, Tritchler DL, Yaffe MJ. Mammographic densities and breast cancer risk. Cancer Epidemiol Biomarkers Prev 1998;7:1133–1144. [PubMed: 9865433]
18. Tice JA, Cummings SR, Ziv E, Kerlikowske K. Mammographic breast density and the gail model for breast cancer risk prediction in a screening population. Breast Cancer Res Treat 2005;94:115–122. [PubMed: 16261410]
19. Barlow WE, White E, Ballard-Barbash R, et al. Prospective breast cancer risk prediction model for women undergoing screening mammography. J Natl Cancer Inst 2006;98:1204–1214. [PubMed: 16954473]
20. Chen J, Pee D, Ayyagari R, et al. Projecting absolute invasive breast cancer risk in white women with a model that includes mammographic density. J Natl Cancer Inst 2006;98:1215–1226. [PubMed: 16954474]
21. Hobson, K. Density Danger: Women with dense breasts have a greater likelihood of cancer. US News & World Report; 2007.
22. Pisano ED, Gatsonis C, Hendrick E, et al. Diagnostic performance of digital versus film mammography for breast-cancer screening. N Engl J Med 2005;353:1773–1783. [PubMed: 16169887]
23. Heine JJ, Velthuizen RP. A statistical methodology for mammographic density detection. Med Phys 2000;27:2644–2651. [PubMed: 11190946]
24. Vachon CM, Brandt KR, Ghosh K, et al. Mammographic breast density as a general marker of breast cancer risk. Cancer Epidemiol Biomarkers Prev 2007;16:43–49. [PubMed: 17220330]
25. Chow CK, Venzon D, Jones EC, Premkumar A, O'Shaughnessy J, Zujewski J. Effect of tamoxifen on mammographic density. Cancer Epidemiol Biomarkers Prev 2000;9:917–921. [PubMed: 11008909]
26. Stone J, Gunasekara A, Martin LJ, Yaffe M, Minkin S, Boyd NF. The detection of change in mammographic density. Cancer Epidemiol Biomarkers Prev 2003;12:625–630. [PubMed: 12869401]
27. Heine JJ, Deans SR, Velthuizen RP, Clarke LP. On the statistical nature of mammograms. Med Phys 1999;26:2254–2265. [PubMed: 10587206]
28. Heine JJ, Deans SR, Cullers DK, Stauduhar R, Clarke LP. Multiresolution statistical analysis of high-resolution digital mammograms. IEEE Trans Med Imaging 1997;16:503–515. [PubMed: 9368106]
29. Heine JJ, Behera M. Aspects of signal-dependent noise characterization. J Opt Soc Am A Opt Image Sci Vis 2006;23:806–815. [PubMed: 16604760]
30. Berg WA, Campassi C, Langenberg P, Sexton MJ. Breast Imaging Reporting and Data System: inter- and intraobserver variability in feature analysis and final assessment. AJR Am J Roentgenol 2000;174:1769–1777. [PubMed: 10845521]
31. Hanley JA, McNeil BJ. The meaning and use of the area under a receiver operating characteristic (ROC) curve. Radiology 1982;143:29–36. [PubMed: 7063747]
32. Freedman AN, Seminara D, Gail MH, et al. Cancer risk prediction models: a workshop on development, evaluation, and application. J Natl Cancer Inst 2005;97:715–723. [PubMed: 15900041]
33. Fenton JJ, Taplin SH, Carney PA, et al. Influence of computer-aided detection on performance of screening mammography. N Engl J Med 2007;356:1399–1409. [PubMed: 17409321]
34. Weitzel JN, Buys SS, Sherman WH, et al. Reduced mammographic density with use of a gonadotropin-releasing hormone agonist-based chemoprevention regimen in BRCA1 carriers. Clin Cancer Res 2007;13:654–658. [PubMed: 17255289]
35. Cuzick J, Warwick J, Pinney E, Warren RM, Duffy SW. Tamoxifen and breast density in women at increased risk of breast cancer. J Natl Cancer Inst 2004;96:621–628. [PubMed: 15100340]

36. Vachon CM, Pankratz VS, Scott CG, et al. Longitudinal trends in mammographic percent density and breast cancer risk. Cancer Epidemiol Biomarkers Prev 2007;16:921–928. [PubMed: 17507617]
37. Boyd N, Martin L, Stone J, Little L, Minkin S, Yaffe M. A longitudinal study of the effects of menopause on mammographic features. Cancer Epidemiol Biomarkers Prev 2002;11:1048–1053. [PubMed: 12376506]
38. Boyd NF, Greenberg C, Lockwood G, et al. Effects at two years of a low-fat, high-carbohydrate diet on radiologic features of the breast: results from a randomized trial. Canadian Diet and Breast Cancer Prevention Study Group. J Natl Cancer Inst 1997;89:488–496. [PubMed: 9086005]
39. Heine, JJ.; Kaufhold, J. Comparing two breast density metrics for risk assessment. In: Peitgen, H-O., editor. IWDM 2002: 6th International Workshop on Digital Mammography; June 22–25 2002; Bremen, Germany: Springer; 2002. p. 544-546.
40. Ferrari RJ, Rangayyan RM, Desautels JE, Borges RA, Frere AF. Identification of the breast boundary in mammograms using active contour models. Med Biol Eng Comput 2004;42:201–208. [PubMed: 15125150]
41. Ojala T, Nappi J, Nevalainen O. Accurate segmentation of the breast region from digitized mammograms. Comput Med Imaging Graph 2001;25:47–59. [PubMed: 11120407]
42. Bick U, Giger ML, Schmidt RA, Nishikawa RM, Wolverton DE, Doi K. Automated segmentation of digitized mammograms. Acad Radiol 1995;2:1–9. [PubMed: 9419517]
43. Pisano ED, Gatsonis CA, Yaffe MJ, et al. American College of Radiology Imaging Network digital mammographic imaging screening trial: objectives and methodology. Radiology 2005;236:404–412. [PubMed: 15961755]

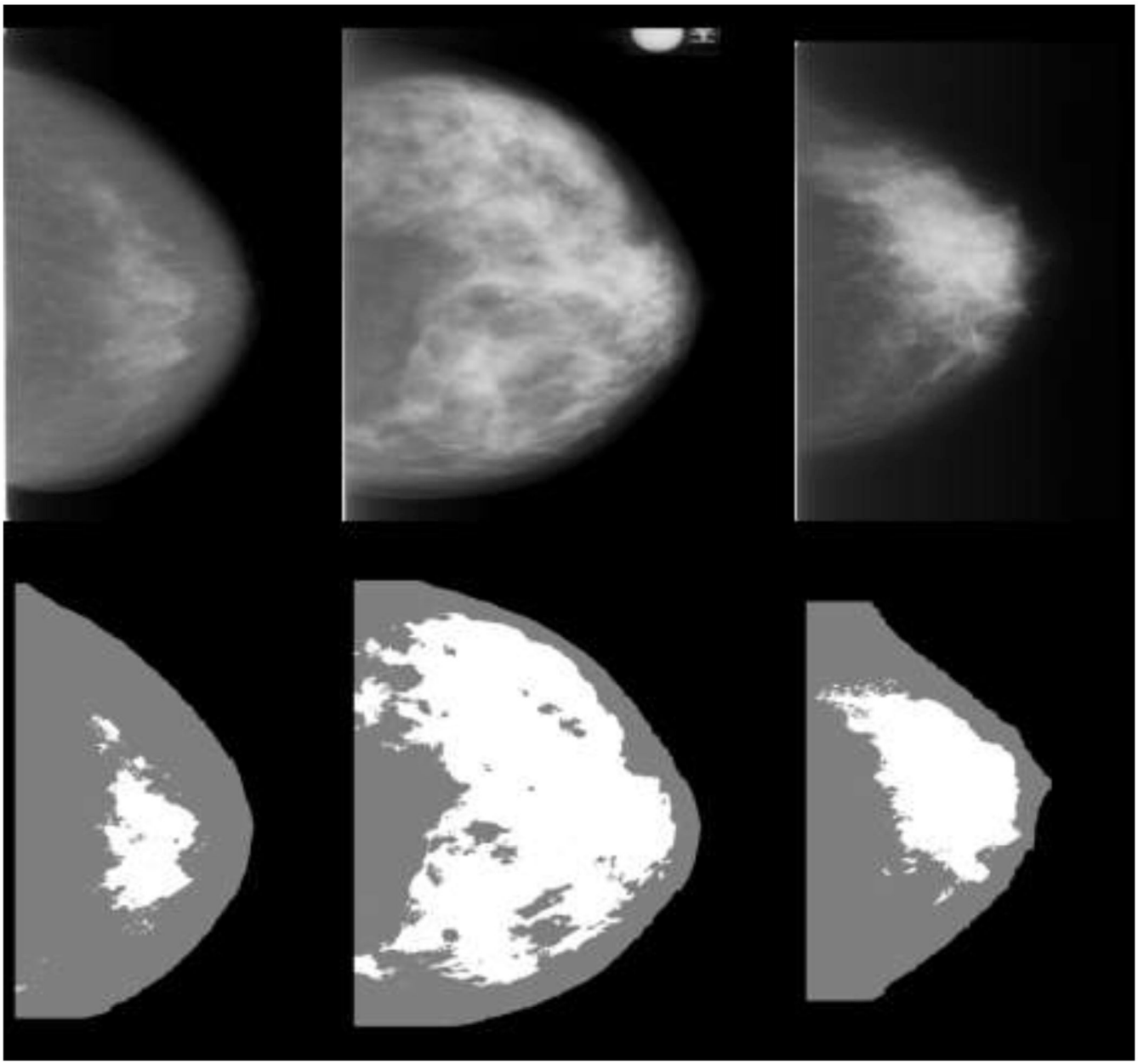

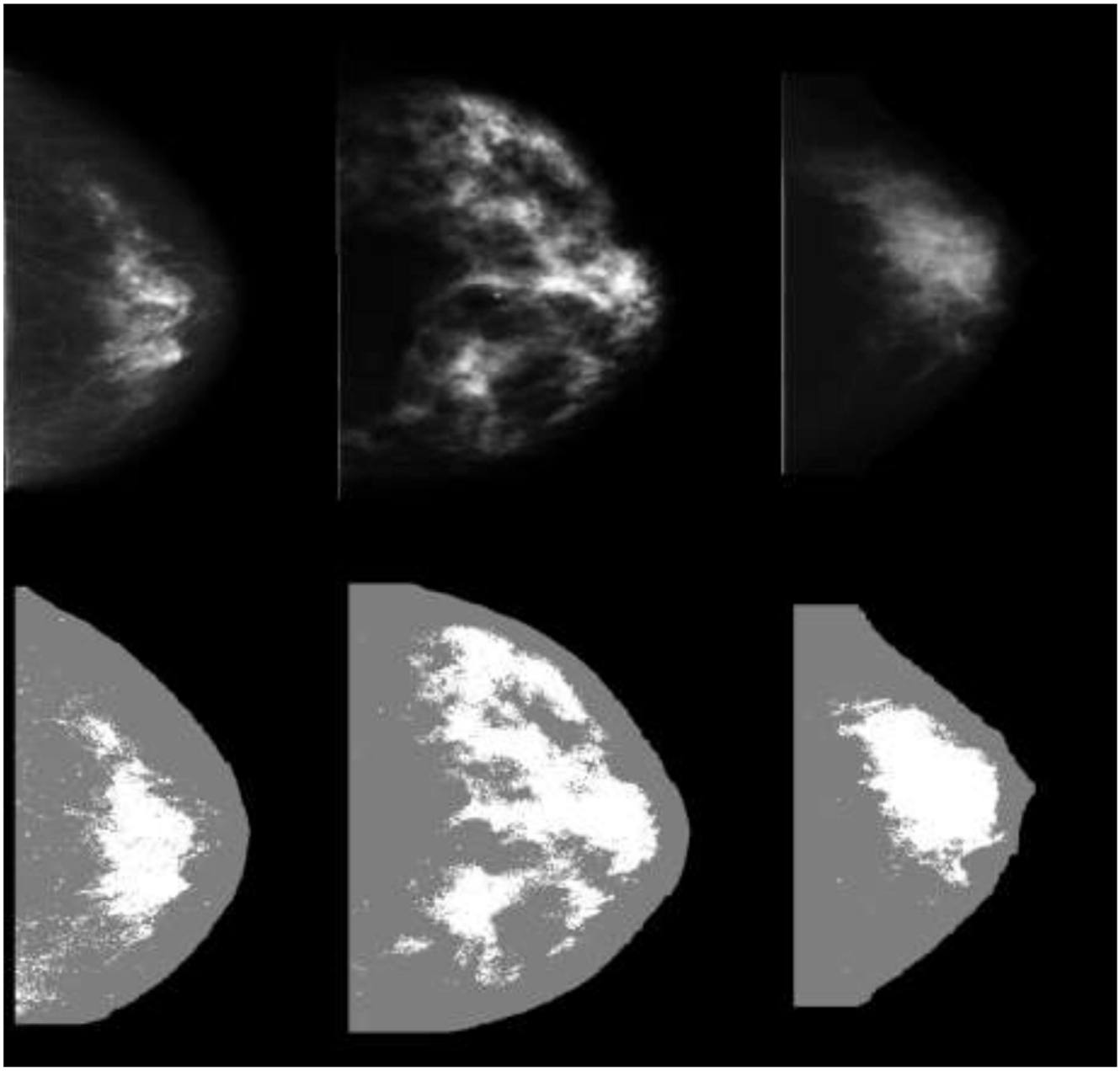

Fig. 1.

1a—Craniocaudal (CC) mammogram images displayed in the LS-75 representation (top row) and the corresponding CM density (PD) labeled images (bottom row) for three women with varying densities from left to right are 13%, 56%, and 28%.

1b—Craniocaudal (CC) mammogram images displayed in the converted digital (DBA) representation (top row) and the corresponding ABDM density (PD_A) detected images (bottom row) for three women with varying densities from left to right are 18%, 24%, and 21%.

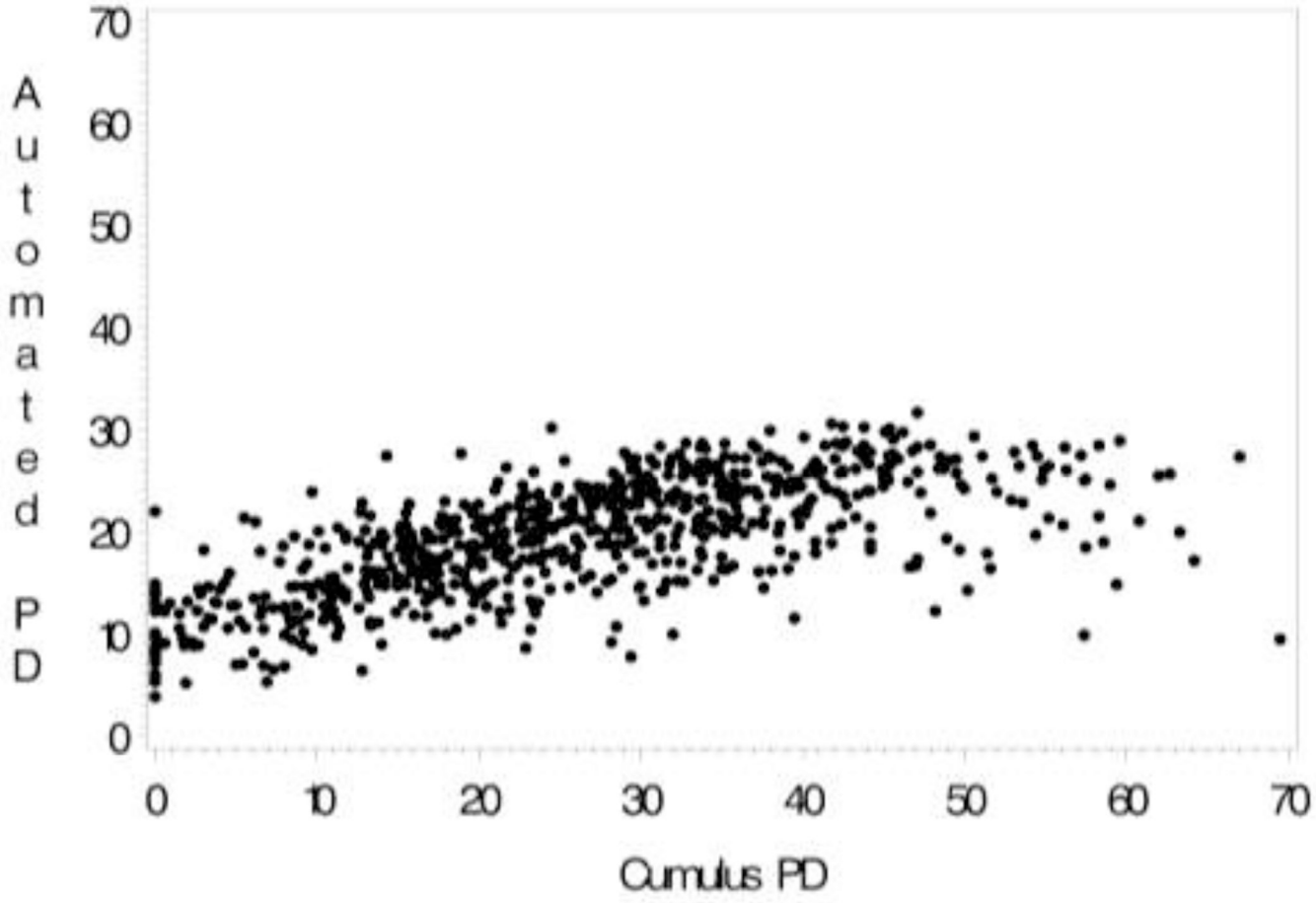

Fig. 2.
The correlation between CM (PD)-ABDM (PD_A) for craniocaudal (CC) mammogram view among 703 controls

Table 1

Description of matching variables and percent density (CM) for cases and controls

Characteristic	Case *n*	Case Mean (SD) or %	Control *n*	Control Mean (SD) or %	p-value
Matching variables					
Age at earliest mammogram (years)	372	61.33 (10.36)	713	61.06 (10.03)	0.70
Interval between early and late mammograms (years)	372	7.05 (1.51)	713	6.99 (1.48)	0.53
Number of screening mammograms	372	5.01 (1.45)	713	5.18 (1.79)	0.11
Residence (% Olmsted County)	183	49.59%	365	51.19%	0.49
Postmenopausal at earliest mammogram	312	84.32%	582	82.44%	0.44
Percent density (PD)*					
Ipsilateral side					
Mediolateral Oblique View	366	28.42 (14.43)	705	24.48 (13.77)	<0.001
Craniocaudal View	366	30.55 (14.09)	701	26.63 (14.74)	<0.001
Contralateral side					
Mediolateral Oblique View	364	27.95 (14.22)	707	24.38 (13.54)	<0.001
Craniocaudal View	363	30.76 (14.46)	703	26.62 (14.56)	<0.001

* The total case/control patient numbers vary from the top portion of the table in comparison with the image numbers used for the PD analysis as only cases and controls with both CM and ABDM measures were used in these analyses.

Table 2

Mean PD_A (ABDM) and PD (CM) by BI-RADS category for controls only.* Contralateral side

		PD_A (ABDM)		PD (CM)	
BI-RADS Category	**N Controls**	**Mean (SD) CC view**	**Mean (SD) MLO view**	**Mean (SD) CC view**	**Mean (SD) MLO view**
1	254	16.6 (5.1)	16.4 (4.5)	16.8 (11.0)	15.8 (10.2)
2	78	17.5 (5.0)	17.8 (4.2)	21.3 (11.1)	18.7 (9.3)
3	182	21.1 (4.5)	20.8 (4.3)	31.7 (12.0)	29.0 (11.6)
4	198	23.0 (4.6)	22.2 (4.6)	36.2 (13.5)	33.1 (12.9)
All categories		19.6 (5.5)	19.3 (5.1)	26.5 (14.6)	24.3 (13.6)
r†		0.49	0.48	0.57	0.56

*707 controls were used for the BI-RADS, PD and PD_A MLO analyses and 703 controls for CC analyses.

†Spearman correlation coefficient.

Table 3

Association of breast cancer risk factors and percent density assessed by three methods. Controls only*

	Mean (SD)		%
Variable	**PD_A (ABDM)**	**PD (CM)**	**BI-RADS 4**
Age			
<50	23.0 ± 4.6	35.9 ± 13.8	45.2%
50–59	20.3 ± 5.8	28.7 ± 14.9	36.3%
60–69	18.5 ± 5.3	23.3 ± 13.7	19.8%
70+	17.7 ± 4.9	21.9 ± 12.0	15.1%
BMI Quartiles			
17.1 – 23.5	21.5 ± 4.7	35.5 ± 14.9	42.6%
23.6 – 26.1	20.0 ± 5.2	27.7 ± 12.2	28.6%
26.2 – 29.9	19.0 ± 5.8	24.1 ± 13.2	20.1%
30.0 – 53.7	17.9 ± 5.6	19.3 ± 12.7	18.7%
Menopausal status			
Premenopausal	22.9 ± 4.6	35.4 ± 13.8	47.6%
Postmenopausal	18.9 ± 5.4	24.8 ± 14.0	23.6%
Postmenopausal Hormones			
Never	19.2 ± 5.5	25.4 ± 14.7	24.4%
Ever	20.8 ± 5.4	30.4 ± 13.8	35.5%
Unknown	17.8 ± 4.7	21.5 ± 12.3	28.6%
1st degree Family History Breast Cancer			
None	19.7 ± 5.5	27.1 ± 14.7	28.4%
Positive	18.9 ± 5.5	23.0 ± 12.9	23.0%
Parity			
Nulliparous	20.7 ± 5.0	32.4 ± 13.8	32.2%
1–2 children	20.0 ± 5.6	28.4 ± 14.9	32.6%
3+ children	19.1 ± 5.6	24.3 ± 14.1	24.0%

*PD and PD_A assessed from CC view from contralateral side of 703 controls. BI-RADS estimated using both CC and MLO view.

Table 4

Association of Percent Density with Risk of Breast Cancer for the BI-RADS, CM and ABDM Method[*] Contralateral Side[↑,‡]

BI-RADS				CM (PD)					ABDM (PD_A)		
Category	**Case/ Control**	**OR (95%)**	**AUC**	**View**	**Quartile PD or PD_A[§,//]**	**Case/ Control**	**OR (95%)**	**AUC**	**Case/ Control**	**OR (95%)**	**AUC**
1	92/254	1.00 (reference)	0.61	CC	1	56/175	1.00 (reference)	0.63	41/178	1.00 (reference)	0.64
2	43/78	1.58 (1.01–2.48)			2	87/176	1.69 (1.13–2.53)		81/172	2.31 (1.47–3.64)	
3	86/182	1.49 (1.04–2.14)			3	90/176	2.10 (1.37–3.22)		100/178	3.02 (1.94–4.70)	
4	148/198	2.61 (1.82–3.75)			4	130/176	3.81 (2.42–5.99)		141/175	5.18 (3.26–8.20)	
					Continuous[**]		1.67 (1.42–1.97)	0.64		1.79 (1.53–2.10)	0.64
				MLO	1	57/175	1.00 (reference)	0.60	36/175	1.00 (reference)	0.64
					2	98/178	1.83 (1.23–2.74)		75/179	2.53 (1.56–4.10)	
					3	96/175	2.00 (1.32–3.05)		114/179	4.48 (2.76–7.27)	
					4	113/179	2.82 (1.81–4.40)		139/174	6.14 (3.74–10.08)	
					Continuous[**]		1.56 (1.33–1.83)	0.63		1.89 (1.61–2.23)	0.64

[*] All models were adjusted for age and body mass index.

[↑] For all models, p-values from tests for trend were < 0.001.

[‡] Numbers of cases and controls are the same for analyses of PD and PD_A performed within CC (363 cases, 703 controls) and MLO (364 cases, 707 controls) views. Numbers of cases and controls for BI-RADS analyses were 369 cases and 712 controls.

[§] Cutpoints for quartiles of CM percent density (PD) for craniocaudal (CC) view are 15.8, 25.8, 35.6 and for mediolateral oblique (MLO) view are 14.5, 23.7, 32.7.

[//] Cutpoints for quartiles for ABDM percent density (PD_A) for CC view are 15.4, 20.1, 23.9 and for MLO view are 15.7, 19.4, 23.0.

[**] Continuous PD and PD_A assessments correspond to a one standard deviation increase. SDs are 14.6 and 13.5 for PD from CC and MLO views and 5.5 and 5.1 for PD_A from CC and MLOs.